Indian Journal of Natural Products and Resources
Vol. 14(3), September 2023, pp 409-424
DOI: 10.56042/ijnpr.v14i3.5397

Green tea as SIRT1 and SIRT3 activator in COVID-19: A molecular docking approach

Hasnat Khan, Shivangi Patel and Anuradha Majumdar*

Department of Pharmacology, Bombay College of Pharmacy, Kalina, Mumbai 400098, India

Received 16 December 2021; revised received 21 August 2023; accepted 25 August 2023

This study reports docking analysis and performance of catechin and its derivatives in activating the SIRT1 and SIRT3 protein for the treatment of COVID-19. Val-412, Asp-348, Pro-271, and Ser-442 are interactions involved in hydrogen bonding and Ile-316, Ala 262, Ile-347, Val-445, Phe-297, His 363 are interactions involved in hydrophobic bonding between the various ligands and SIRT1 protein. ILE-111, Val-173, Asp-112, Phe-38 are interactions involved in hydrogen bonding and Phe-38, Ala-27, Ile-111, His-129, Phe-38 are involved in hydrophobic bonding between the various ligands and SIRT3 protein. Catechin gallate and epigallocatechin gallate show promising potential as SIRT1 activators as observed by their binding affinity ΔG=-10.9 kcal/mol and ΔG=-10.6 kcal/mol, which are lower than the binding affinity of the standard therapeutic moiety resveratrol (ΔG=-9.0 kcal/mol). All catechins show promising potential as SIRT3 activators, as revealed by their binding affinities, which are lower than the binding affinity of the standard therapeutic moiety resveratrol (ΔG=-8.4 kcal/mol). Amongst all the catechins, catechin gallate shows 61.53% binding site similarity with the native ligand in the case of SIRT1 protein. Amongst all the catechins, epicatechin and epigallocatechin show 100% binding site similarity with the native ligand for the SIRT3 protein. Therefore, we suggest that catechins can serve as SIRT1 and SIRT3 activators, which may prove to be a possible therapy for COVID-19.

Keywords: Binding affinity, Catechins, COVID-19, SIRT1, SIRT3

IPC code; Int. cl. (2021.01)– A61K 36/00

Introduction

Severe acute respiratory syndrome coronavirus-2 (SARS-CoV-2) caused the coronavirus disease 2019 (COVID-19) which affects multiple organs. It was declared a pandemic in March 2020 by The World Health Organization (WHO), with about 571,678 confirmed cases and 26,494 deaths globally around that time[1]. Various mutations of the virus and a high rate of transmission, thus leading to high mortality rates, are all a result of the second wave of the disease. There is no particular COVID-19 treatment which is very effective, and it is the need of the hour to search for more reliable and natural treatments to curb the pandemic.

For the virus to enter the host cell and its subsequent replication in the host, a combination of factors comes into play. Numerous conformational changes are necessary for the successful binding and entry of an encapsulated virus into a host cell[2]. The oxidant/antioxidant balance determines the redox status of a host cell, which is responsible for contributing to the proteins' stability and interactions occurring at the host cell surface[3]. Furthermore, after the virus has successfully entered the host, the innate immune system recognises the foreign genome and responds by activating macrophages and dendritic cells They then use reactive oxygen/nitrogen radicals and cytokines, which can contribute to inflammation and aggravate the host system response in favour of COVID-19[4] progression. As a result, the possible consequences of oxidative stress vs 'cytokine storm'-induced inflammation and the role of natural antioxidants in preventing fatal results should be examined and explored[1].

Growing evidence points to Sirtuin 1's (SIRT1) role in the pathogenesis of COVID-19. P53 and proinflammatory cytokine levels are elevated in COVID-19 patients, but SIRT1 expression in peripheral blood mononuclear cells is decreased[5]. According to a recent study, SIRT1 is necessary for the (D-Ala2)-dynorphin 1-6 (leytragin), a peptide agonist of δ-opioid receptors, to have an inhibitory effect on high mobility group box 1 (HMGB1) production in the lungs of mice with acute lung injury

*Correspondent author
Email: anuradha.majumdar@bcp.edu.in; anuradha.majumdar@gmail.com

brought on by lipopolysaccharide (LPS)[6]. The clinical severity of COVID-19 being closely correlated with extracellular HMGB1, leytragin-induced SIRT1 activation may aid in the creation of HMGB1-targeting treatments and, consequently, in the prevention of the cytokine storms that frequently accompany COVID-19. SIRT1, which increases expression of the gene that codes for tissue metalloproteinase inhibitor 3 (TIMP3), downregulates ADAM 17 (A Disintegrin and Metalloproteinase Domain 17), also known as TNF-α-converting enzyme (TACE), which is of highest relevance[7]. The levels of Tumour Necrosis Factor alpha (TNF-α), Interleukin 1(IL-1), and Interleukin 6 (IL-6) consequently drop. When TNF-α levels rise, SIRT1 inhibits ADAM 17, which in turn regulates TNF-α synthesis in a negative feedback loop that indirectly affects the production of TNF-α dependent IL-1 and IL-6[7]. TNF-α and IL-6 are released if SIRT1 does not suppress the production of ADAM17, which may result in an uncontrolled hyperinflammatory response like COVID-19[7,8]. SIRT1 has anti-inflammatory properties via inhibiting ADAM17 and, subsequently, TNF-α and IL-6. By using the Fenton reaction (Fe2+ + H2O2 Fe3+ + HO% + OH), which transforms active iron (Fe2+) to its inert form (Fe3+), which is stored in hepatocytes and macrophages as well as ferritin, increased ADAM17 attempts to mitigate tissue injury in cases of severe oxidative stress. Additionally, this may convert haemoglobin into methaemoglobin, decreasing its ability to bind to oxygen[9,10].

Along with the Sirtuin family (SIRT1-7) and the control and modification of the inflammatory response, SIRT1 serves as the first line of defence against DNA and RNA viral infections[11]. SIRT1 encourages autophagy which reduces apoptosis and offers defence against hypoxic stress in various respiratory infections and cardiovascular disorders. Increased SIRT1 activity immediately reduces viral replication and prevents activation of ADAM17, which lowers TNF-α, IL-1, and IL-6 levels. In contrast, SIRT1 depletion promotes viral replication while inhibiting ADAM17 function minimally or not at all, leading to an unchecked rise in TNF-α, IL-6, and IL-1 levels. In the absence of NAD+ or Zn++, SIRT1 would not be sufficiently activated, leading to an unregulated increase in TNF-α which would typically boost SIRT1 activity to downregulate ADAM17. Given the previous information, it is probable that activation of SIRT1 may be essential for a successful defense against viral infection and may avoid the hyperinflammatory response[9,12]. Additional studies into the SIRT1 activators' potential to reduce excessive inflammatory responses may reveal a therapeutic approach for the acute lung injury and cytokine storms frequently connected to COVID-19 disease[13]. The literature does not prove the direct contribution of Sirtuin 3 (SIRT3) in the inhibition of SARS-COV2 virus replication. However, it mediates its antioxidant effects via its interaction with Manganese Superoxide Dismutase (MnSOD) and isocitrate dehydrogenase 2 (IDH2) and may be a potential target for intervention therapy against COVID-19.

According to history, tea leaves steeped in boiling water have been consumed since at least 500,000 years ago[14]. The botanical evidence suggests that India and China were among the first countries to cultivate tea. Green tea has been proven to have significant health benefits, and it is already used by hundreds of millions of people around the world[14]. The leaves of the *Camellia sinensis* plant are used to make green tea. This plant, first cultivated in East Asia, can grow as large as a shrub or tree. *C. sinensis* can be found all across Asia, as well as regions of the Middle East and Africa[14]. Green tea, which is made up of unfermented leaves, is said to have the highest concentration of powerful antioxidants known as polyphenols[15]. Many chemicals, such as free radicals created by the body and environmental poisons, such as UV rays from the sun, are combined. Antioxidants, such as the polyphenols in green tea, can neutralise free radicals, reducing or even preventing part of the damage they produce in COVID-19 pathogenesis[16].

Further, we go on to emphasize the role of the various catechins like epicatechin, epigallocatechin, epicatechin gallate, and epigallocatechin gallate as SIRT-1 and SIRT-3 activators and also prove via molecular docking approach how they elevate the antioxidant enzymes mainly SOD and GSH that are compromised in case of COVID-19[17]. Therefore, this can help attenuate further ROS generation and scavenge the already-formed ROS. This would throw some light on the role of catechins in the treatment of COVID-19.

Chemical constituents of green tea

The health benefits posed by green tea are because they contain the most powerful antioxidants, the

polyphenols[15]. In comparison, it has been found that polyphenols have stronger antioxidant effects than Vitamin C. Polyphenols present in green tea, known as catechins[15], impart a bitter flavour. Epicatechin, epigallocatechin, epicatechin gallate, and epigallocatechin gallate (EGCG) are four primary catechins in green tea[18]. Antioxidant, anticarcinogenic, anti-inflammatory, thermogenic, probiotic, and antimicrobial properties in various *in vitro* studies, *in vivo* studies and reports on humans are attributed to polyphenols[19,20]. Amongst all 4, the most abundant and active is EGCG. Alkaloids like caffeine, theobromine, and theophylline are present too in green tea, which contribute to its stimulant effects. All the tea types contain constituents which surmount their antibacterial and antioxidant properties, which go on to decrease as the colour of the tea becomes darker and darker because of the presence of lower content of oxidizing polyphenols in the leaves[21].

Chemistry of catechins and their potential antioxidant activity

Catechins belong to the flavonoid family, and they are also called flavan-3-ols or flavanols. The chemical structure of catechin comprises a dihydropyran heterocycle (C-ring), with carbon 3 having the hydroxyl group and two benzene rings(A and B). Two chiral centres of the molecule are present on carbons 2 and 3[22]. Flavan-3-ol compounds are those catechin stereoisomers in *cis* -(−)-epicatechin or *trans* -(+)-catechin configuration, with respect to carbons 2 and 3[22]. Esterification with gallate groups leads to flavanols forming gallic acid conjugates such as epicatechin gallate (ECG), epigallocatechin (EGC), and epigallocatechin gallate (EGCG)[22]. Catechin polymerisation leads to condensed catechins[22]. A-type and B-type procyanidins are the common oligomers derived out of epicatechins. In A-type dimers, the monomers are linked by both a 4→8 carbon–carbon and a 2→O7 ether bond, and the monomers of the B-type dimers are linked through 4→8 carbon–carbon bonds[22].

Catechins can create and scavenge free radicals, demonstrating their positive benefits through a mix of processes[23]. Catechins' antioxidant activity is mediated in two ways: (1) direct mechanisms and (2) indirect mechanisms. Direct processes include scavenging ROS and chelating metal ions, whereas indirect mechanisms include antioxidant enzymes activation, inhibition of pro-oxidant enzymes, and synthesis of phase II detoxification enzymes and antioxidant enzymes[24]. Catechins and their diastereoisomers contain phenolic hydroxyl groups, which are important for stabilizing free radicals. The direct antioxidant effects of catechins enable themto function as free radical scavengers. If the phenolic hydroxyl groups of catechins combine with reactive oxygen and nitrogen species in a termination reaction, the cycle of radical formation can be stopped. There is a reduction of free radicals after catechins give one electron of the phenolic OH group, and the aromatic group can be formed. This aromatic group can now maintain stability by resonance of the resultant aroxyl radicals[25]. A radical form of the antioxidant is produced after interaction with the former reactive species, which thereafter undergoes stabilization by charge delocalization brought about by the interaction of the phenolic hydroxyl groups with the π-electrons of the benzene ring. The extent of structure conjugation and the number and arrangement of hydroxyl groups determines the antioxidant potential of phenolic compounds[26]. EGCG > ECG > EGC > EC > C represents the relative hierarchy of effectiveness of catechins as radical scavengers[27]. Therefore, cellular lipids are prevented from undergoing oxidation as catechins serve as free radical scavengers and stop radical chain reactions.

The ability of the phenolic compounds to chelate metal ions, leading to the generation of free radicals, contributes to their antioxidant capacity. Iron chelation sites are often the adjacent hydroxyl groups present in the molecule. Regulation of protein synthesis and signaling pathways is also brought about by catechins because of their antioxidant potential. In a study, significantly elevated activities of superoxide dismutase (SOD), catalase (CAT), and glutathione peroxidase (GSH)[28], playing crucial roles in scavenging ROS, were observed when mice were given 0.2% catechins. In another study, it was observed that two weeks of consumption of green tea led to the induction of catalase expression in the aorta of spontaneously hypertensive rats[29]. Elevation of plasma and tissue glutathione levels in several animal studies was brought about by green tea[30].

Inhibition of pro-oxidant enzymes, e.g., NADPH (nicotinamide adenine dinucleotide phosphate)-oxidase, or modulation of interaction of ligands with receptors, e.g., TNF-α and suppression of oxidative stress-related pathways responsible for the

inflammation processes are brought about by catechins. They also bring about the modulation of activities of redox-sensitive transcription factors-nuclear factor kappa-light-chain-enhancer of activated B cells (NF-κB) and activator protein-1 (AP-1), which play a vital role in pathogenesis-related to oxidative stress response.

Catechins can interact with membranes in two ways: by adsorption or penetration into lipid bilayers. Because of the interaction of their hydrophobic benzene rings with protein proline residues and the hydrogen-bonding capability of the phenolic hydroxyl groups, phenolic structures have a significant ability to interact with proteins. As a result of catechins being structurally similar to ATP, they can bind to the enzyme's ATP-binding sites competitively. The structural/conformational characteristics of catechins and hydrogen bonding are responsible for catechin interactions with transcriptional factors.

Sirtuins are NAD+-dependent type III histone deacetylases with yeast SIR2 as their founding component and whose major function is to silence gene expression by histone deacetylation[31]. Apart from histone in the mitochondria, mammalian sirtuins target various proteins in the cytoplasm and mitochondria. The sirtuin family has seven members in mammals (SIRT1–7). SIRT1, SIRT6, and SIRT7 are found in thenucleus; SIRT2 is found in the cytoplasm; and mitochondria[32] contains SIRT3, SIRT4, and SIRT5. Based on sequence homology, class I sirtuins include SIRT1, SIRT2, and SIRT3, which have deacetylase activity.

Role of SIRT-1 in activating antioxidant defenses

SIRT1 operates as a metabolic sensor by deacetylating key transcription factors and cofactors in response to changes in energy status. SIRT1 regulates mitochondrial activity and biogenesis, as well as oxidative stress, inflammation, apoptosis, and cellular senescence. Bordoni *et al*.[5] found that the deacetylase SIRT1 expression was lower in COVID-19 patients and was adversely linked with p53. In COVID-19 patients, their findings revealed that the inflammatory environment and the dysregulated p53/SIRT1 axis might impact cell survival, B cell signaling, and antibody production.

Role of SIRT3 in activating antioxidant defenses

SIRT3 is known to be attributed to long lifespan in humans because of its mitochondrial localisation. Mitochondrial enzymes involved in fatty acid β-oxidation, amino acid metabolism, the electron transport chain (ETC), and antioxidant defenses are deacetylated and activated by SIRT3 too[33,34]. Some studies claim that SIRT3 is located exclusively in mitochondria[34], but other studies carried out by different labs proved the presence of SIRT3 in the nucleus and cytoplasm too[35]. SIRT3 is present in the inner mitochondrial membrane cristae and the matrix within the mitochondria[34].

Conversion of $O\bullet^{-2}$ to H_2O_2, which is further converted to water by catalase, is carried out by MnSOD[36]. Deacetylation of MnSOD in mitochondria is carried out by SIRT3, significantly enhancing its ability to scavenge ROS[37]. Also, an increase in the activity of IDH2 is seen due to its deacetylation brought by SIRT3[38]. An enzyme of the tricarboxylic acid cycle, IDH2, produces NADPH, a molecule known to cause regeneration of antioxidants. Furthermore, the reduction of thiol groups of oxidized proteins is brought about by Glutathione (GSH). GSH can be regenerated by oxidized glutathione (GSSG) with the help of glutathione reductase, which is NADPH-dependent. Elevated levels of NADPH are produced due to enhanced activity of IDH2 by SIRT3-mediated deacetylation, which in turn helps increase the activity of glutathione reductase to further facilitate regeneration of GSH from GSSG. Transcription of oxidative stress response genes is promoted by SIRT3. Cell metabolism and generation of a response to oxidative stress are regulated by members of the fork head box subgroup O (FOXO) transcription factors. Transcription of catalase and MnSOD is facilitated by SIRT3 binding to FoxO3a[39]. In a study, it has been found that mRNA levels of both MnSOD and catalase are increased by over expression of SIRT3 in mouse cardiomyocytes[40]

Material and Methods

Protein preparation

The three-dimensional protein structures of SIRT1 and SIRT3 were obtained from www.rcsb.org with PDB ID 4ZZJ and 4JT8, respectively. The proteins were prepared by removing water molecules and heteroatoms, followed by conversion to .pdb format using BIOVIA Discovery Studio Visualizer v20.1.0.19295. Then the protein structures were further processed by adding polar hydrogen atoms and Kollman charges on them, this was done in

Autodock Vina, followed by conversion of the pdb structure to the pdbqt structure in the same.

Ligand preparation

The chemical structure of catechin and its derivatives, along with standard resveratrol, were retrieved from the PubChem database (https://pubchem.ncbi.nlm.nih.gov/) in the spatial Data File(.sdf) format. Chemical structures of ligands in the .sdf format were converted to the .pdb format using BIOVIA Discovery Studio Visualizer. Ligand structures were also prepared by adding non-polar hydrogens, Gasteiger charges, and rotatable bonds and converted in .pdbqt format using Autodock Vina.

Active site selection

Active site determination was done for the SIRT1 protein (PDB ID:4ZZJ) with the help of an open server, "The Achilles Blind Docking server". After the completion of the blind docking, several conformers were generated, out of which the conformer with the least energy was selected for further studies, and the co-ordinates of that conformer were noted down (11.83, 61.02, 24.75) in this case. These co-ordinates were further used to generate the first grid box with dimensions (60, 60, 60). After this, the conformer with the lowest energy was selected after docking for the actual study.

Grid box selection

SIRT1

The grid box was based on the conformer with the lowest energy after docking. The Grid box was selected with the help of Autodock Vina, and the parameters were noted down. The co-ordinates of origin were set as x=9.998, y=60.921, and z=25.928,with box size of x=34,y=30, and z=24. This was based on the location of the native ligand on the protein of the lowest conformer.The number of modes and exhaustiveness were set at 10 and 12, respectively.

SIRT3

The grid box was selected based on the location and binding of the native ligand (1NR) with the protein. The grid box was selected with the help of Autodock Vina, and the parameters were noted down. The co-ordinates of origin were set as x=22.751, y=42.520 and z=-10.830, with box size of x=12, y=32, and z=28. This was based on the location of the native ligand on the protein. The number of modes and exhaustiveness were set at 10 and 12, respectively.

Docking using Autodock Vina

The docking simulation of the ligands and protein was performed using Autodock Vina.

Grid box and docking validation

The grid box generated with the help of a native ligand further needs to be validated to see if the dimensions of the grid box we have provided are correct or not. For this validation, the native ligands (4TQ) and (1NR), in the case of SIRT1 and SIRT3, respectively, were removed from the complex and then redocked into the active site using the dimensions of the grid box with the help of AutoDock Vina. It was done by opening the co-crystallized complex in Notepad^{++}, removing the heteroatoms of the ligand from the complex and then saving it as a different file in PDB format. This was done to ensure that the ligand binds exactly to the active site cleft and does not show much deviation when compared to the actual co-crystallized complex. The redocked complex was then superimposed to the original complex using Pymol 2.3, the root mean square deviation (RMSD) was calculated, and the 2D image of the interactions was taken to see if the interactions were the same.

Visualising interactions

BIOVIA Discovery Studio 3.5, UCSF Chimera 1.13.1, and PyMOL 2.3 were used to visualize and study the 2D and 3D ligand interactions with the protein.

Results

Before conducting the docking simulations, it is important to check the likeliness of a compound as a drug using the Lipinski criteria. Based on Lipinski criteria, the molecular weight of the compound must be less than 500 g/mol, the maximum number of donor atoms is 5, the maximum number of acceptor atoms is 10, and the value of log P must be below 5. The molecular weight of the compounds epicatechin, epigallocatechin, catechin gallate and epigallocatechin gallate are 290.26, 306.27, 442.4, and 458.37 g/mol, respectively. The log P values of compounds epicatechin, epigallocatechin, catechin gallate, and epigallocatechin gallate are 1.80, 1.49, 1.5, and 1.49,

respectively. It was found that catechin and its derivatives mostly fulfilled those requirements and thus can be further evaluated using molecular docking simulations. The docking simulations were performed on 6 ligands viz: Native ligand (4TQ) = Control (in case of SIRT1); Native ligand (1NR) (in case of SIRT3); Resveratrol = Standard; Epicatechin; Epigallocatechin; Catechingallate; Epigallocatechingallate. The binding sites of the native ligand on the SIRT1 protein involve 1 non-conventional hydrogen bond and 13 other hydrophobic bonding (Table 1,3 and Fig. 1a–b). The control (native ligand) (4TQ) has been successfully docked on SIRT1 protein with the binding affinity score of -11.6 kCal/mol, as given in Table 3. The binding sites of the native ligand on the SIRT3 protein involve 6 non-conventional hydrogen bonds and 4 other hydrophobic bonding (Table 2,4 and Fig. 2a–b). The control (native ligand) (1NR) has been successfully docked on SIRT3 protein with the binding affinity score of -9.9 kCal/mol as given in Table 4. The standard (resveratrol) ligand has been successfully docked on SIRT1 protein with the binding affinity score of -9.0 kCal/mol, as given in Table 3. The standard (resveratrol) ligand has been successfully docked on SIRT3 protein with the binding affinity score of -8.4 kCal/mol, as given in Table 4. The binding sites of resveratrol on the SIRT1 protein involve 2 conventional hydrogen bonds and 5 other hydrophobic bonding (Table 5 and Fig. 3a–b). The binding sites of resveratrol on the SIRT3 protein involved 2 conventional hydrogen bonds and 5 other hydrophobic bonding (Table 5 and Fig. 4a-b). The epicatechin (ligand 1) has been successfully docked with SIRT1 protein with the binding affinity score of -8.7 kCal/mol, as given in Table 3. The epicatechin (ligand 1) has been successfully docked with SIRT3 protein with the binding affinity score of -8.9 kCal/mol, as given in Table 4. The binding sites of epicatechin on the SIRT1 protein involve 2 conventional hydrogen bonds and 4 other hydrophobic bonds (Table 5 and Fig. 5a–b), and the binding sites of epicatechin on the SIRT3 protein involve 3 conventional hydrogen bonds and 4 other hydrophobic bonds (Table 5 and Fig. 6a–b). Epigallocatechin (ligand 2) has been successfully docked with SIRT1 protein with the binding affinity score of -8.7 kCal/mol as given in Table 3.

Table 1 — Hydrogen bonding of native ligand with SIRT1 protein

Amino acid of protein	Atom of protein	Atom of ligand	Bond distance in Aº
Val-412	Oxygen	Hydrogen	3.33

Table 2 — Hydrogen bonding of native ligand with SIRT3 protein

Amino acid of protein	Element of protein	Atom of Ligand	Bond distance in Aº
Asp 112	Oxygen	Hydrogen	2.03
Ile 111	Hydrogen	Oxygen	2.21
Phe 38	Hydrogen	Nitrogen	2.23
Asp 112	Hydrogen	Oxygen	2.27
Val 173	Oxygen	Hydrogen	2.36
Ile 111	Hydrogen	Sulphur	2.75

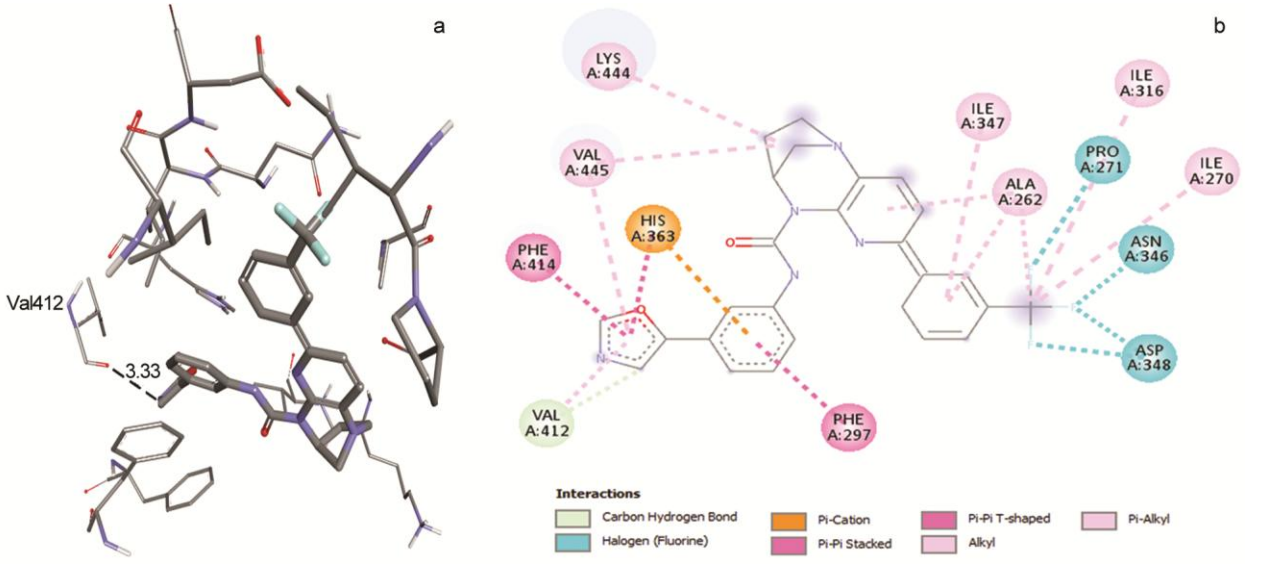

Fig. 1 — a) Interaction of native ligand (4TQ) with SIRT1 protein forming hydrogen bond; and b) Interaction of native ligand (4TQ) with SIRT1 protein forming hydrophobic bond.

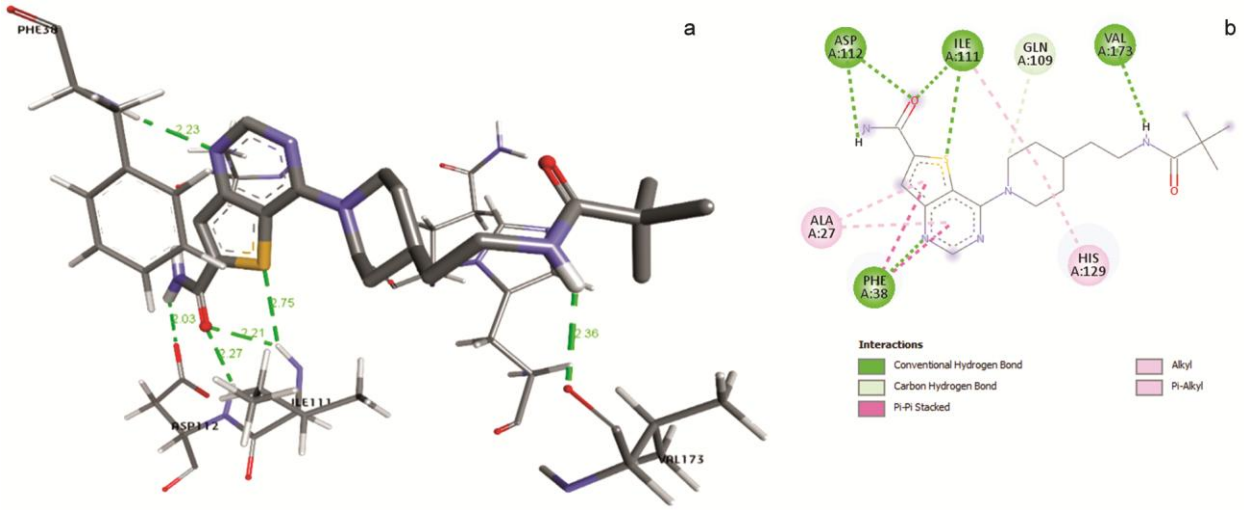

Fig. 2 — a) Interaction of native ligand (1NR) with SIRT3 protein forming hydrogen bond; and b) Interaction of native ligand (1NR) with SIRT3 protein forming hydrophobic bond.

Table 3 — Docking simulation results in case of SIRT1 protein

Test ligand	Hydrogen bond length (A)	Residue involved in hydrogen bonding	Functional group of ligand	Residue involved in hydrophobic interaction	Binding site similarity to native ligand %	Binding affinity kCal/mol
1NR (Native ligand)	2.03	Asp 112	Hydrogen(-NH)	Phe-38	100%	-9.9
	2.21	Ile 111	Oxygen(-COO)	Ala-27		
	2.23	Phe 38	Nitrogen(-NH)	Ile-111		
	2.27	Asp 112	Oxygen(-COO-)	His-129		
	2.36	Val 173	Hydrogen(-NH)			
	2.75	Ile 111	Sulphur(-S-)			
Resveratrol	2.29	Val 173	Hydrogen(OH)	Phe-38	83.3333	-8.4
	2.52	Phe 38	Oxygen(OH)	Ala-27		
				Ile-111		
				His-129		
Epicatechin	2.10	Ile 111	Oxygen(OH)	Phe-38	100%	-8.9
	2.30	Asp 112	Hydrogen(OH)	Ala-27		
	2.54	Val 173	Hydrogen(OH)	Ile-111		
				His-129		
Epigallocatechin	2.09	Ile 111	Oxygen(OH)	Phe-38	100%	-9.0
	2.18	Asp 112	Hydrogen(OH)	Ala-27		
	2.82	Val 173	Hydrogen(OH)	His-129		
Catechin gallate	2.03	Pro 36	Hydrogen(OH)	Phe-38	66.6666	-10.7
	2.96	Arg 39	Oxygen(-C00)	Ala-27		
				His-129		
				Ile-111		
				Phe-61		
Epigallocatechin gallate	2.61	Ala 27	Oxygen(COO)	Ala-27	66.6666	-10.1
	2.66	Val 173	Hydrogen(OH)	Phe-38		
	2.84	Thr 201	Hydrogen(OH)	His-129		

Epigallocatechin (ligand 2) has been successfully docked with SIRT3 protein with the binding affinity score of -9.0 kCal/mol, as given in Table 4. The binding sites of epigallocatechin on the SIRT1 protein involve 3 conventional hydrogen bonds and 3 other hydrophobic bonds (Table 5 and Fig. 7a–b). The

Table 4 — Docking simulation results in case of SIRT3 protein

Test ligand	Hydrogen bond length (A)	Residue involved in hydrogen bonding	Functional group of ligand	Residue involved in hydrophobic interaction	Binding site similarity to native ligand %	Binding affinity kCal/mol
1NR (Native ligand)	2.03	Asp 112	Hydrogen(-NH)	Phe-38	100%	-9.9
	2.21	Ile 111	Oxygen(-COO)	Ala-27		
	2.23	Phe 38	Nitrogen(-NH)	Ile-111		
	2.27	Asp 112	Oxygen(-COO-)	His-129		
	2.36	Val 173	Hydrogen(-NH)			
	2.75	Ile 111	Sulphur(-S-)			
Resveratrol	2.29	Val 173	Hydrogen(OH)	Phe-38	83.3333	-8.4
	2.52	Phe 38	Oxygen(OH)	Ala-27		
				Ile-111		
				His-129		
Epicatechin	2.10	Ile 111	Oxygen(OH)	Phe-38	100%	-8.9
	2.30	Asp 112	Hydrogen(OH)	Ala-27		
	2.54	Val 173	Hydrogen(OH)	Ile-111		
				His-129		
Epigallocatechin	2.09	Ile 111	Oxygen(OH)	Phe-38	100%	-9.0
	2.18	Asp 112	Hydrogen(OH)	Ala-27		
	2.82	Val 173	Hydrogen(OH)	His-129		
Catechin gallate	2.03	Pro 36	Hydrogen(OH)	Phe-38	66.6666	-10.7
	2.96	Arg 39	Oxygen(-C00)	Ala-27		
				His-129		
				Ile-111		
				Phe-61		
Epigallocatechin gallate	2.61	Ala 27	Oxygen(COO)	Ala-27	66.6666	-10.1
	2.66	Val 173	Hydrogen(OH)	Phe-38		
	2.84	Thr 201	Hydrogen(OH)	His-129		

binding sites of epigallocatechin on the SIRT3 protein involve 2 conventional hydrogen bonds and 5 other hydrophobic bonds (Table 5 and Fig. 8a–b). Catechingallate (ligand 3) has been successfully docked on SIRT1 protein with the binding affinity score of -10.9 kCal/mol as given in Table 3. Catechin gallate (ligand 3) has been successfully docked on SIRT3 protein with the binding affinity score of -10.7 kCal/mol, as given in Table 4. The binding sites of catechin gallate on the SIRT1 protein involve 4 conventional hydrogen bonds and 5 other hydrophobic bonds (Table 3 and Fig. 9a–b).The binding sites of catechin gallate on the SIRT3 protein involve 2 conventional hydrogen bonds and 5 other hydrophobic bonds (Table 4 and Fig. 10a–b). Epigallocatechin gallate (ligand 4) has been successfully docked with SIRT1 protein with a binding affinity score of -10.6 (Table 3 and Fig. 11a–b). Epigallocatechin gallate (ligand 4) has been successfully docked with SIRT3 protein with the binding affinity score of -10.1 kCal/mol, as given in Table 4. The binding sites of the epigallocatechin gallate on the SIRT1 protein involve 4 conventional hydrogen bonds and 7 other hydrophobic bonds (Table 4,5). The binding sites of the epigallocatechin gallate on the SIRT3 protein involve 3 conventional hydrogen bonds and 4 other hydrophobic bonds (Table 4,5 and Fig. 12a–b).

Revalidation in case for SIRT1 protein was conducted by examining the binding affinity of its native ligand into the active pocket. It was seen that the native ligand was bound exactly to the same active site with a binding score of -11.6 kCal/mol. Val-412, Ile-270, Ile-316, Ala-262, Ile-347, Lys-444, Val-445, Phe-414, His-363, Pro-271, Asp-346, and Asp-348 are the interacting amino acids in the active site pocket and totally 1 non-conventional hydrogen bond was formed with a threshold of 4.00 Aº. The redocked complex was then superimposed on the native co-crystallized protein using BIOVIA Discovery Studio Visualizer, and a low RMSD of 0.0510 Aº was observed (Fig. 13a). Further, revalidation in case for SIRT3 protein was conducted by examining the binding affinity of its native ligand into the active

Table 5 — Hydrogen bonding of ligands with concerned protein's amino acid involved, atom of ligand involved and bond distance

Hydrogen bonding	Amino acid of protein	Atom of protein	Atom of ligand	Bond distance in Aº
Resveratrol with SIRT1 protein	Val-412	Oxygen	Hydrogen	2.23
	Asp-348	Oxygen	Hydrogen	2.60
Resveratrol with SIRT3 protein	Val 173	Oxygen	Hydrogen	2.29
	Phe 38	Hydrogen	Oxygen	2.52
Epicatechin with SIRT1 protein	Asp-348	Oxygen	Hydrogen	1.92
	Val-412	Oxygen	Hydrogen	2.35
Epicatechin with SIRT3 protein	Ile 111	Hydrogen	Oxygen	2.10
	Asp 112	Oxygen	Hydrogen	2.30
	Val 173	Oxygen	Hydrogen	2.54
Epigallocatechin with SIRT1 protein	Ile 111	Hydrogen	Oxygen	2.09
	Asp 112	Oxygen	Hydrogen	2.18
	Val 173	Oxygen	Hydrogen	2.82
Epigallocatechin with SIRT3 protein	Pro-271	Oxygen	Hydrogen	2.09
	Ser-265	Hydrogen	Oxygen	3.73
Catechin gallate with SIRT1 protein	Pro-271	Oxygen	Hydrogen	1.83
	Asp-348	Oxygen	Hydrogen	2.08
	Ser-442	Hydrogen	Oxygen	2.14
	Ser-441	Oxygen	Hydrogen	2.26
Catechin gallate with SIRT3 protein	Pro 36	Oxygen	Hydrogen	2.03
	Arg 39	Hydrogen	Oxygen	2.96
Epigallocatechin gallate with SIRT1 protein	Val-412	Oxygen	Hydrogen	1.82
	Pro-271	Oxygen	Hydrogen	1.96
	Ser-442	Hydrogen	Oxygen	2.40
	Ala-262	Hydrogen	Oxygen	2.81
Epigallocatechin gallate with SIRT3 protein	Ala 27	Hydrogen	Oxygen	2.61
	Val 173	Oxygen	Hydrogen	2.66
	Thr 201	Oxygen	Hydrogen	2.84

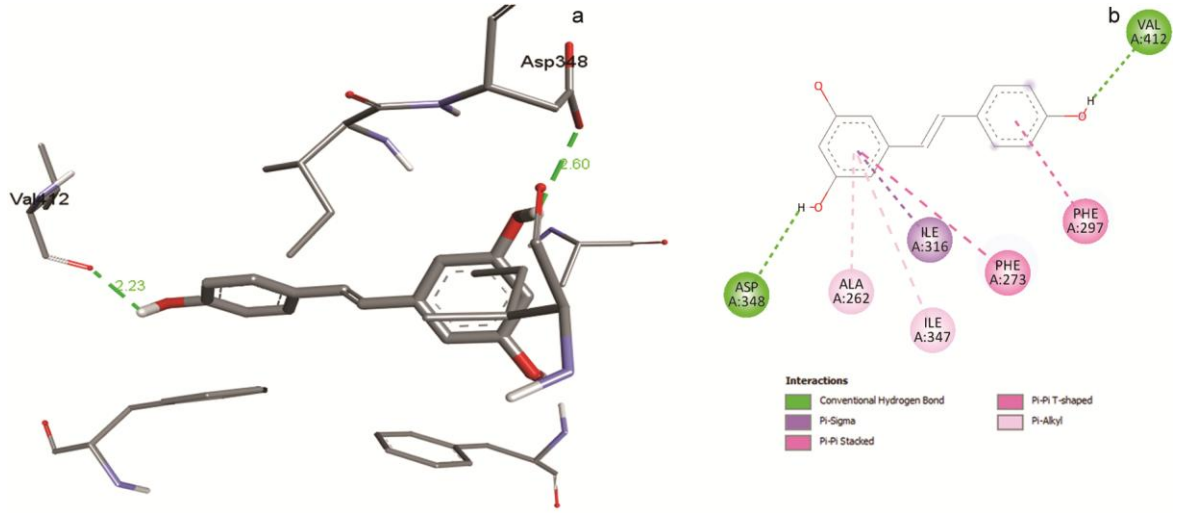

Fig. 3 — a) Interaction of resveratrol with SIRT1 protein forming hydrogen bond; and b) Interaction of resveratrol with SIRT1 protein forming hydrophobic bond.

pocket. The native ligand was found to be bound exactly to the same active site with a binding score of -9.9 kCal/mol. Phe-38, Ala-27, Ile-111, His-129, Asp-112, and Val-173 were the interacting amino acids in the active site pocket, and six hydrogen bonds were formed with a threshold of 3.00 Aº. The redocked complex was then superimposed on the native co-crystallized protein using BIOVIA Discovery Studio Visualizer, and a low RMSD of 0.510 Aº was observed (Fig. 13b).

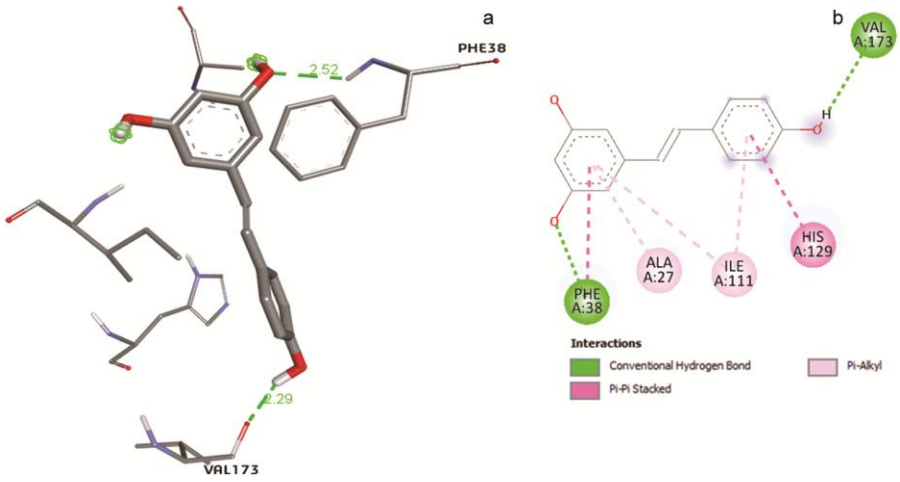

Fig. 4 — a) Interaction of resveratrol with SIRT3 protein forming hydrogen bond; and b) Interaction of resveratrol with SIRT3 protein forming hydrophobic bonds.

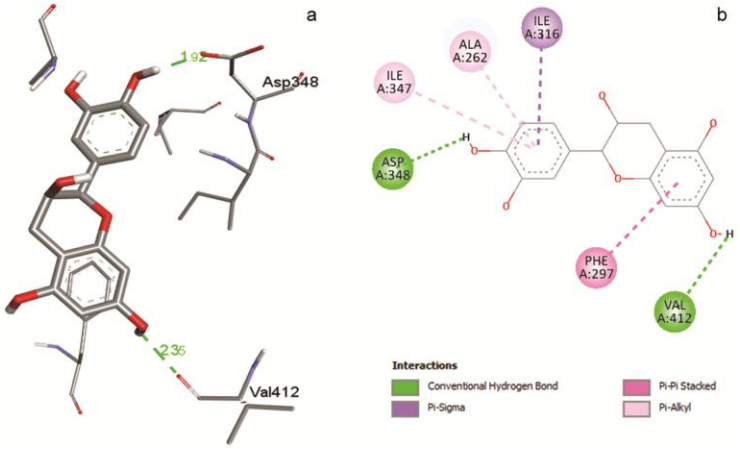

Fig. 5 — a) Interaction of epicatechin with SIRT1 protein forming hydrogen bond; and b) Interaction of epicatechin with SIRT1 protein forming hydrophobic bond.

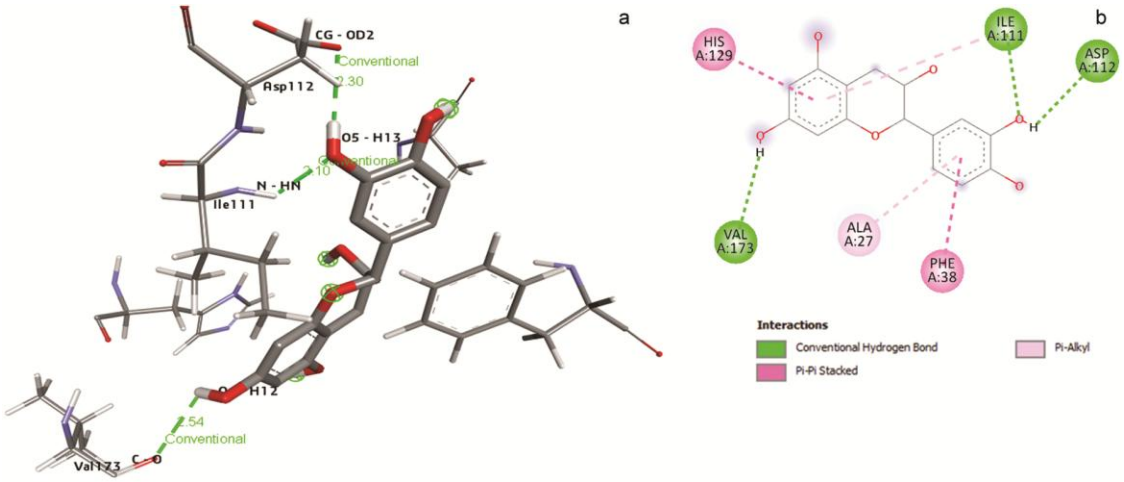

Fig. 6 — a) Interaction of epicatechin with SIRT3 protein forming hydrogen bond; and b) Interaction of epicatechin with SIRT3 protein forming hydrophobic bond.

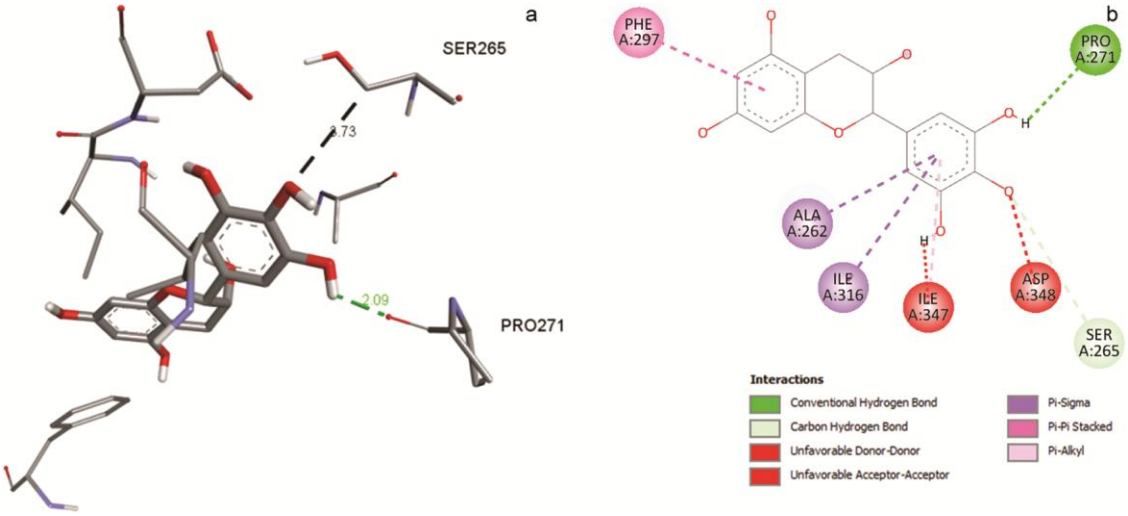

Fig. 7 — a) Interaction of epigallocatechin with SIRT1 protein forming hydrogen bond; and b) Interaction of epigallocatechin with SIRT1 protein forming hydrophobic bond.

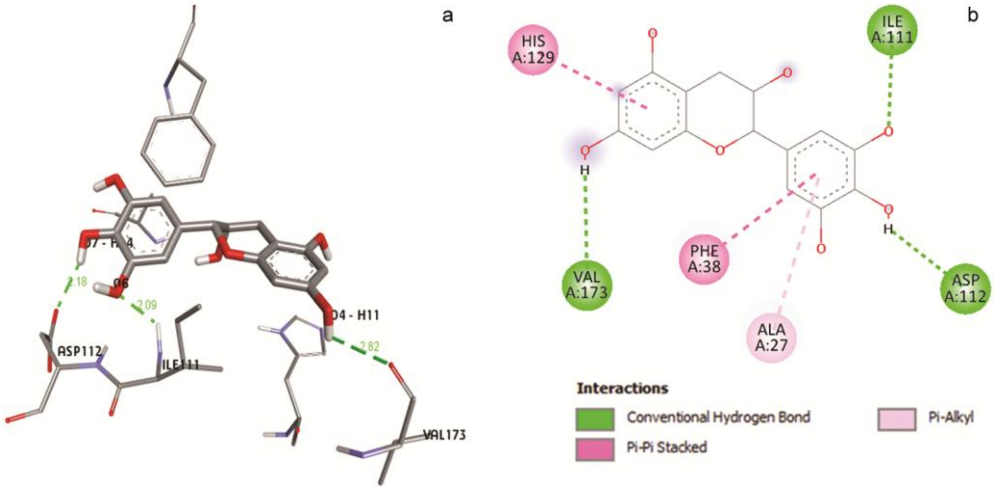

Fig. 8 — a) Interaction of epigallocatechin with SIRT3 protein forming hydrogen bond; and b) Interaction of epigallocatechin with SIRT3 protein forming hydrophobic bonds.

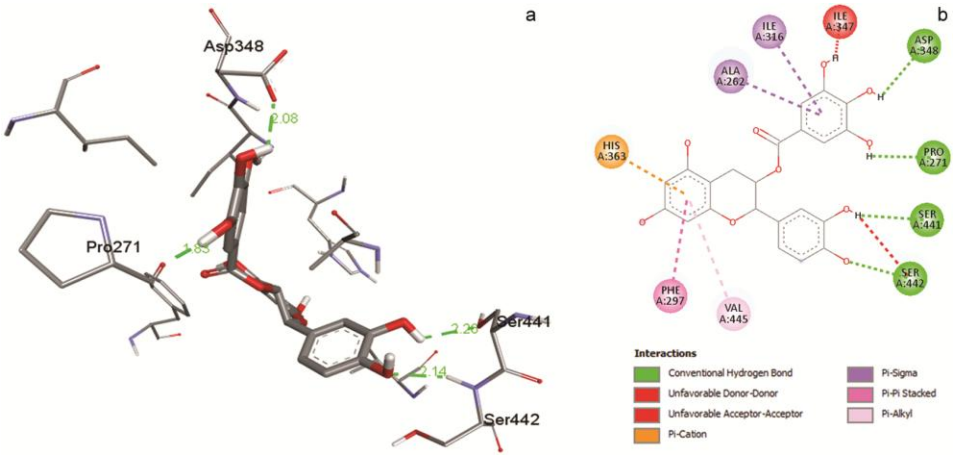

Fig. 9 — a) Interaction of catechin gallate with SIRT1 protein forming hydrogen bond; and b) Interaction of catechin gallate with SIRT1 protein forming hydrophobic bond.

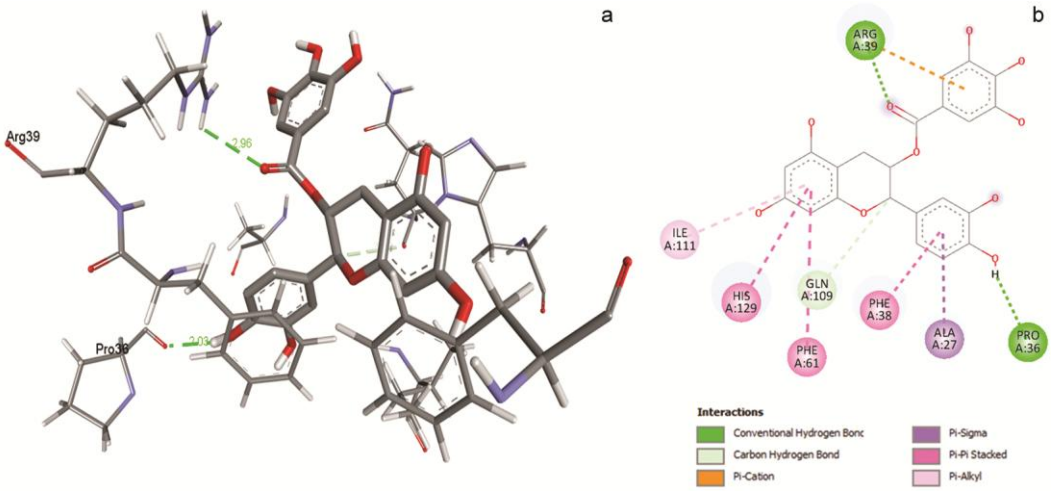

Fig. 10 — a) Interaction of catechin gallate with SIRT3 protein forming hydrogen bond; and b) Interaction of catechin gallate with SIRT3 protein forming hydrophobic bond.

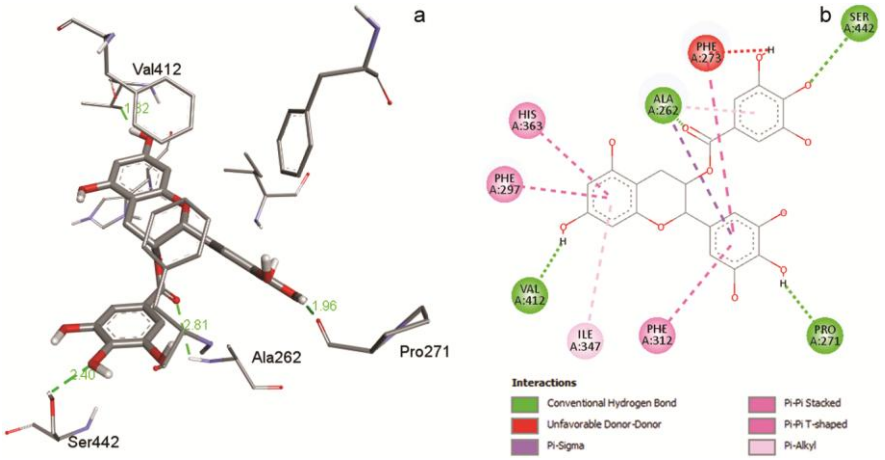

Fig. 11 — a) Interaction of epigallocatechin gallate with SIRT1 protein forming hydrogen bond; and b) Interaction of epigallocatechin gallate with SIRT1 protein forming hydrophobic bond.

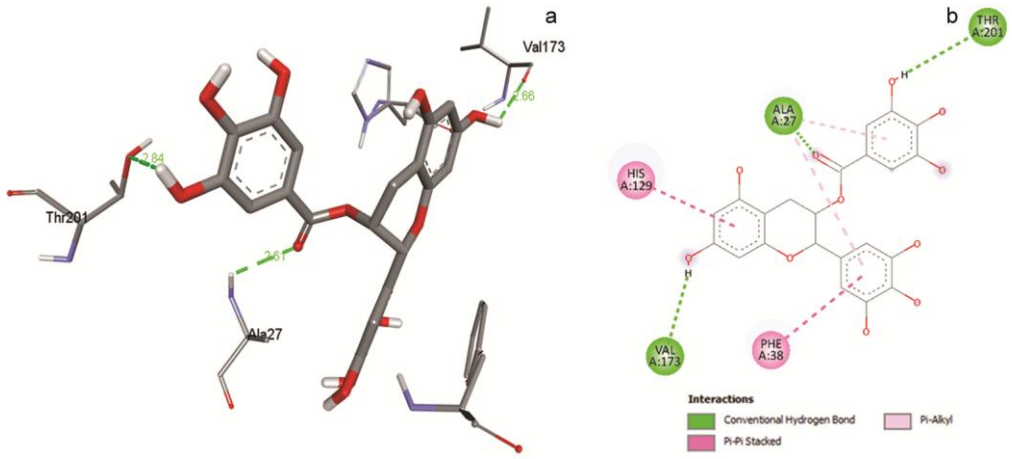

Fig. 12 — a) Interaction of epigallocatechin gallate with SIRT3 protein forming hydrogen bond; and b) Interaction of epigallocatechin gallate with SIRT3 protein forming hydrophobic bond.

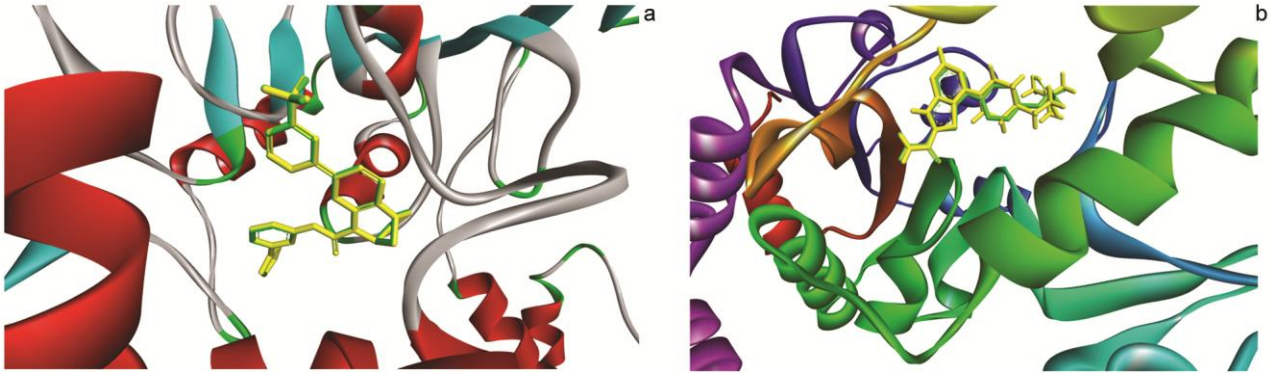

Fig. 13 — a) Redocking (in case of SIRT1). In the figure, green represents native ligand and yellow represents docked ligand; and b) Redocking (in case of SIRT3). In the figure, green represents native ligand and yellow represents docked ligand.

Discussion

With reference to SIRT1, the docking simulation results for the native ligand (redocking) show the binding affinity ΔG as -11.6 kCal/mol, which can be seen in the figure of docking simulation (Fig. 13a). The binding of the native ligand (4TQ) includes only one non-conventional hydrogen bond and 13 other hydrophobic bonds. The non-conventional hydrogen bond is weak, with a bond length of 3.33Aº formed with the oxygen of Val-412 with the hydrogen of –CH of the ligand. Other residues involved in hydrophobic interactions are listed in the docking simulation Table 3. Apart from these interactions, other interactions are also formed with the fluorine of the native ligand, known as halogen bonds. Pro-271, Asn-346 and Asp-348 are the three amino acids involved in halogen bonding with the fluorine of the ligand. One pi-cation is formed with His-363. The binding of resveratrol, as standard, shows ΔG=-9.0 kCal/mol forming 2 hydrogen bonds and 5 hydrophobic bonds. The strongest hydrogen bond between Val-412 of protein with hydrogen (OH) of ligand, having a bond length of 2.23Aº. The other hydrogen bond between Asp-348 of protein and oxygen (OH) of the ligand is slightly weaker, having a bond length of 2.60 Aº. When compared with native ligand in terms of bonding and with respect to pocket region present in protein, there is almost 46.153% similarity to the native ligand and suggests that it fits in almost the same pocket region as the native ligand, losing some hydrophobic interactions like Ile-270, Lys-444, Val-445, Phe-414, His-363, and some bonds with Pro-271 and Asp-346 while forming hydrogen bond with Asp-348. The decrease in affinity energy is due to the loss of many hydrophobic interactions compared to native ligands. The binding of epicatechin shows ΔG=-8.7 kCal/mol, forming 2 hydrogen bonds and 4 other hydrophobic bonds. The strongest hydrogen bond is between ASP-348 of the protein with hydrogen (OH) of the ligand having a bond length of 1.92Aº; the other bond formed is slightly weak, between Val-412 of the protein with hydrogen (OH) of the ligand with a bond length of 2.35Aº. For epicatechin, the pocket binding region is significantly the same as for resveratrol; it retains almost all the interactions shown by resveratrol, but in comparison to the native ligand, it has only 46.15% similarity, like resveratrol. The only interaction that is not present is Phe-273, which is present in resveratrol as a hydrophobic interaction. Other all interactions are similar to resveratrol. The loss of Phe-273 interaction leads to a significant reduction in binding affinity compared to resveratrol. For epigallocatechin, the binding affinity is ΔG=-8.7 kCal/molforming 2 hydrogen bonds, 1 conventional and 1 non-conventional bond. The conventional hydrogen bond is stronger, having a bond length of 2.09Aº, formed between Pro-271 of protein with hydrogen (OH) of the ligand. The non-conventional bond is weaker, with a bond length of 3.73Aº formed between Ser-265 of protein with oxygen (OH)of the ligand. The hydrogen bond with Ser-265 is a new bond that is not seen with any other ligand apart from this ligand. The similarity percentage is 46.153% when compared to the native ligand. The similarity score is much the same as resveratrol, but the type of bonds differ. Two unfavourable interactions are responsible for a decrease in the binding affinity. Catechin gallate binds with a binding score of ΔG= -10.9 kCal/mol, forming four hydrogen bonds and 5 other hydrophobic bonds. Also, three other interactions are observed, including two unfavourable interactions (Ile-347 and Ser-442) and pi-cation (His-363). The strongest hydrogen bond is formed with Pro-271 of the protein with hydrogen (OH) of the

ligand with a bond length of 1.83Aº, and the weakest one is formed with Ser-441 of the protein with hydrogen (OH) of the ligand.Two new hydrogen bonds were seen at Ser-442 and Ser-441, which were not seen before with any of the ligands. The similarity percentage is 61.53% compared to the native ligand, showing very much the same binding pocket; two unfavourable interactions along with one pi-cation interaction are mainly responsible for decreased binding affinity. Epigallocatechin gallate binds with a binding score of ΔG=-10.6 kCal/mol, forming four hydrogen bonds and 7 hydrophobic bonds. Only one unfavourable interaction is seen with Phe-273. The strongest bond is seen with Val-412 of the protein with hydrogen (OH) of the ligand having a bond length of 1.82Aº, and the weakest is with Ala-262 of the protein with oxygen (COO) of the ligand. Ser-442 and Pro-271 are other residues of the protein that are involved in hydrogen bonding. The similarity percentage was 46.15% compared to a native ligand. This shows that the pocket region is somehow similar to the native ligand, and its 4 hydrogen bonds help in increasing the binding affinity.

In the case of SIRT3, the docking simulation results for the native ligand (redocking) show the binding affinity of ΔG as -9.9 kCal/mol which is seen in the figure of docking simulation (Fig. 13b). The binding of the native ligand (1NR) includes 6 hydrogen bonds and 6 hydrophobic bonds. The strongest bonding occurs between Asp-112 and the hydrogen of -NH Group of the ligand with a bond length 2.03 Aº. Other 5 hydrogen bonds are also formed, with the weakest between Ile-111 and the ligand's Sulphur (-S-) having a bond length 2.75 Aº. Other amino acids involved in hydrogen bonding are Phe-38 and Val-173. The binding of resveratrol, as standard, shows ΔG=-8.4, forming 2 hydrogen bonds and 5 hydrophobic bonds. The strongest hydrogen bond is between Val-173 of protein and hydrogen (OH) of ligand, having a bond length of 2.29 Aº. The other hydrogen bond between Phe-38 of protein and oxygen (OH) of the ligand is slightly weaker, having a bond length of 2.52 Aº. When compared with the native ligand in terms of bonding and with respect to the pocket region in protein,there is almost 83.33% similarity to the native ligand, which suggests that it fits in almost the same pocket region as the native ligand. In the case of epicatechin and epigallocatechin, this binding pocket region is the same as for the native ligand, as it retains all the interactions shown by the native ligand, revealing a similarity percentage of 100% when compared to the native ligand. However, the binding affinity for epicatechin and epigallocatechin is -8.9 kCal/mol and -9.0 kCal/mol, respectively. This decrease in the binding affinity of both epicatechin and epigallocatechin is due to the loss of the hydrogen bond, and that hydrogen bond is changed to a hydrophobic bond. Both the molecules depict 3 hydrogen bonds, each with Ile-111, Asp-112 and Val-173, but the bond length is increased in the case of epigallocatechin, thus weakening the bond and henceforth leading to weaker binding affinity. Catechin gallate shows the highest binding affinity with a score of ΔG=-10.7 kCal/mol. Catechin gallate forms only two hydrogen bonds, but both are from different pocket regions compared to the native ligand. The stronger one is with Pro-36 of the protein with hydrogen (OH) of the ligand, and the other one is between Arg-39 of the protein with oxygen (-COO-) of the ligand; the bond length of both the bonds are 2.03 Aº and 2.96 Aº respectively. The hydrophobic bonds occur in the same pocket region as the native ligand, having a similarity score of 66.66%. This high binding affinity is due to the two hydrogen bonds formed from a different pocket region, showing that Pro-36 and Arg-39 are important for increasing the affinity. The last compound here is epigallocatechin gallate, which forms three hydrogen bonds, with the strongest at Ala-27 and the weakest at Thr-201. This hydrogen bond at Thr-201 is mainly responsible for increasing the binding affinity to -10.1 kCal/mol; other than that, all the bonds are similar to native ligands and thus have a similarity score of 66.66%. From the analysis above, the hydrophobic interactions of Phe-38, Ala-27, and His-129 are found to be continuously present in all the ligands. This shows that these three amino acids in the protein form a stable pocket for the compounds to reside and activate the SIRT3 protein. Val-173 plays a major role in locking the functional groups of the compounds (native, resveratrol, epicatechin, epigallocatechin and epigallocatechingallate) in the vicinity of the targeting protein via hydrogen bonding.

Conclusion

Molecular docking simulation of epicatechins and their derivatives on SIRT1 have been performed to explore the potential of these compounds in activating the target. Epicatechin and epigallocatechin have

somewhat the same binding affinity when compared to standard (resveratrol). Catechin gallate and epigallocatechin gallate have higher binding affinity when compared to standard (resveratrol). No catechin derivatives have a higher binding affinity than the native ligand (4TQ). However, among the four catechin derivatives, catechin gallate is shown to be the best activator, followed by epigallocatechin gallate and then epigallocatechin and epicatechin. All four ligands, along with resveratrol in general, have been docked on the same pocket as the native ligand, showing its similarity in biochemistry for SIRT1 activation. This study also reveals that two residues of the SIRT1 protein.

Val-412 and Asp 348 were involved in hydrogen bonds and 5 residues involved in the other interactions (hydrophobic and pi-cation) [Ala-262, Ile-316, Phe-297, Ile-347,H is-363] were crucial in the molecular interactions between catechin derivatives and SIRT1. Other than these interactions, interactions of Pro-271, Ser-442, Ser-441 and Val-445 need to be further investigated as it helps in increasing the binding affinity and thus further stabilizing the complex.

On the other hand, molecular docking simulation of epicatechins and its derivatives on SIRT3 reveals that all four ligands have more binding affinity when compared to standard (resveratrol), but only catechin gallate and epigallocatechin gallate has higher binding affinity when compared to native (control) ligand. Catechin gallate is shown to be the best activator, followed by epigallocatechin gallate, then epigallocatechin and epicatechin. All ligands in general, except catechin gallate and epigallocatechin gallate, have been docked on the same pocket as the native ligand, showing its similarity in biochemistry in the activation of SIRT3. This study also reveals that two residues of the SIRT3 protein (Val-173 and Asp-112) involved in hydrogen bonding and 4 residues involved in the hydrophobic interactions (Phe-38, Ala-27, His-129, Ile-111) are crucial in the molecular interaction between catechins and SIRT3. Other than these interactions, interactions of Pro-36, Arg-39 and Thr-201 need to be further investigated as they might help increase the binding affinity and thus further stabilize the complex.

We propose that catechins can be further evaluated in suitably designed *in vitro* and *in vivo* studies to throw some light on their prospective role in the treatment of COVID-19.

Conflict of interest

The authors declare no conflict of interest.

References

1 Forcados G E, Muhammad A, Oladipo O O, Makama S and Meseko C A, Metabolic implications of oxidative stress and inflammatory process in SARS-CoV-2 pathogenesis: Therapeutic potential of natural antioxidants, *Front Cell Infect Microbiol*, 2021, **11**, 1–11.

2 Suhail S, Zajac J, Fossum C, Lowater H, McCracken C, *et al*., Role of oxidative stress on SARS-CoV (SARS) and SARS-CoV-2 (COVID-19) Infection: A review, *Protein J*, 2020, **39**(6), 644–656.

3 Fenouillet E, Barbouche R and Jones I M, Cell entry by enveloped viruses: Redox considerations for HIV and SARS-coronavirus, *Antioxidants Redox Signal*, 2007, **9**(8), 1009–1034.

4 Bin P, Huang R and Zhou X, Oxidation resistance of the sulfur amino acids: Methionine and cysteine, *Biomed Res Int*, 2017, **2017**, 9584932.

5 Bordoni V, Tartaglia E, Sacchi A, Fimia G M, Cimini E, *et al*., The unbalanced p53/SIRT1 axis may impact lymphocyte homeostasis in COVID-19 patients, *Int J Infect Dis*, 2021, **105**, 49-53.

6 Karkischenko V N, Skvortsova V I, Gasanov M T, Fokin Y V, Nesterov M S, *et al*., Inhaled [D-Ala2]-Dynorphin 1-6 prevents hyperacetylation and release of high mobility group box 1 in a mouse model of acute lung injury, *J Immunol Res*, 2021, **2021**, 1-10.

7 Fontani F, MMPs, ADAMs and their natural inhibitors in inflammatory bowel disease: Involvement of oxidative stress, *J Clin Gastroenterol Treat*, 2017, **3**(1), 1–12.

8 Yoo C H, Yeom J H, Heo J J, Song E K, Lee S l, *et al*., Interferon β protects against lethal endotoxic and septic shock through SIRT1 upregulation, *Sci Rep*, 2015, **4**, 1–8.

9 Miller R, Wentzel A R and Richards G A, COVID-19: NAD+ deficiency may predispose the aged, obese and type 2 diabetics to mortality through its effect on SIRT1 activity, *Med Hypotheses*, 2020, **144**, 110044.

10 Maras J S, Das S, Sharma S, Sukriti S, Kumar J, *et al*., Iron-overload triggers ADAM-17 mediated inflammation in severe alcoholic hepatitis, *Sci Rep*, 2018, **8**(1), 1–14.

11 Budayeva H G, Rowland E A and Cristea I M, Intricate roles of mammalian Sirtuins in defense against viral pathogens, *J Virol*, 2016, **90**(1), 5–8.

12 Khan H, Patel S and Majumdar A, Role of NRF2 and Sirtuin activators in COVID-19, *Clin Immunol*, 2021, **233**, 108879.

13 Kim J K, Silwal P and Jo E K, Sirtuin 1 in host defense during infection, *Cells*, 2022, **11**(18), 2921.

14 Chopade V V, Phatak A A, Upaganlawar A B and Tankar A A, Green tea (*Camellia sinensis*): Chemistry , traditional, medicinal uses and its pharmacological activities- a review, *Pharmacogn Rev*, 2008, **2**(3), 157–162.

15 Craig W J, Health-promoting properties of common herbs, *Am J Clin Nutr*, 1999, **70**(3), 491s-9s.

16 Dulloo A G, Duret C, Rohrer D, Girardier L, Mensi N, *et al.*, Efficacy of a green tea extract rich in catechin polyphenols and caffeine in increasing 24-h energy expenditure and fat oxidation in humans, *Am J Clin Nutr*, 1999, **70**(6), 1040–1045.

17 Muhammad Y, Kani Y A, Iliya S, Muhammad J B, Binji A, *et al*., Deficiency of antioxidants and increased oxidative stress in COVID-19 patients: A cross-sectional comparative study in Jigawa, Northwestern Nigeria, *SAGE Open Med*, 2021, **9**, 205031212199124.

18 McKenna D J, Hughes K and Jones K, Green tea monograph, *Altern Ther Health Med*, 2000, **6**(3), 61–8.

19 Zhong L, Goldberg M S, Gao Y T, Hanley J A, Parent M E, *et al*., A population-based case-control study of lung cancer and green tea consumption among women living in Shanghai, China, *Epidemiology*, 2001, **12**(6), 695–700.

20 Katiyar S K, Afaq F, Perez A and Mukhtar H, Green tea polyphenol (-)-epigallocatechin-3-gallate treatment of human skin inhibits ultraviolet radiation-induced oxidative stress, *Carcinogenesis*, 2001, **22**(2), 287–294.

21 Graham H N, Green tea composition, consumption, and polyphenol chemistry, *Prev Med (Baltim)*, 1992, **21**(3), 334–350.

22 Braicu C, Ladomery M R, Chedea V S, Irimie A and Berindan-Neagoe I, The relationship between the structure and biological actions of green tea catechins, *Food Chem*, 2013, **141**(3), 3282–3289.

23 Oliveira-Marques V, Marinho H S, Cyrne L and Antunes F, Modulation of NF-κB–Dependent gene expression by H2O2: A major role for a simple chemical process in a complex biological response, *Antioxid Redox Signal*, 2009, **11**(9), 2043-2053.

24 Youn H S, Lee J Y, Saitoh S I, Miyake K, Kang K W, *et al*., Suppression of MyD88- and TRIF-dependent signaling pathways of Toll-like receptor by (-)-epigallocatechin-3-gallate, a polyphenol component of green tea, *Biochem Pharmacol*, 2006, **72**(7), 850–859.

25 Bors W, Heller W, Michel C and Saran M, Flavonoids as antioxidants: Determination of radical-scavenging efficiencies, *Methods Enzymol*, 1990, **186**, 343–355.

26 Cao G, Sofic E and Prior R L, Antioxidant and pro-oxidant behavior of flavonoids: Structure-activity relationships, *Free Radic Biol Med*, 1997, **22**(5), 749–760.

27 Fujisawa S and Kadoma Y, Comparative study of the alkyl and peroxy radical scavenging activities of polyphenols, *Chemosphere*, 2006, **62**(1), 71–79.

28 Khan S G, Katiyar S K, Agarwal R and Mukhtar H, Enhancement of antioxidant and phase II enzymes by oral feeding of green tea polyphenols in drinking water to SKH-1 hairless mice: Possible role in cancer chemoprevention, *Cancer Res*, 1992, **52**(14), 4050.

29 Negishi H, Xu J-W, Ikeda K, Njelekela M, Nara Y, *et al*., Black and green tea polyphenols attenuate blood pressure increases in stroke-prone spontaneously hypertensive rats, *J Nutr*, 2004, **134**(1), 38–42.

30 Frei B and Higdon J V, Antioxidant activity of tea polyphenols in vivo: Evidence from animal studies, *J Nutr*, 2003, **133**(10), 3275S-84S.

31 Kincaid B and Bossy-Wetzel E, Forever young: SIRT3 a shield against mitochondrial meltdown, aging, and neurodegeneration, *Front Aging Neurosci*, 2013, **5**, 1–13.

32 Frye R A, Phylogenetic classification of prokaryotic and eukaryotic Sir2-like proteins, *Biochem Biophys Res Commun*, 2000, **273**(2), 793–798.

33 Gurd B J, Holloway G P, Yoshida Y and Bonen A, In mammalian muscle, SIRT3 is present in mitochondria and not in the nucleus; and SIRT3 is upregulated by chronic muscle contraction in an adenosine monophosphate-activated protein kinase– independent manner, *Metab Clin Exp*, 2012, **61**(5), 733–741.

34 Cooper H M and Spelbrink J N, The human SIRT3 protein deacetylase is exclusively mitochondrial, *Biochem J*, 2008, **411**(2), 279–285.

35 Iwahara T, Bonasio R, Narendra V and Reinberg D, SIRT3 functions in the nucleus in the control of stress-related gene expression, *Mol Cell Biol*, 2012, **32**(24), 5022–5034.

36 Spitz D R and Oberley L W, An assay for superoxide dismutase activity in mammalian tissue homogenates, *Anal Biochem*, 1989, **179**(1), 8–18.

37 Qiu X, Brown K, Hirschey M D, Verdin E and Chen D, Calorie restriction reduces oxidative stress by SIRT3-mediated SOD2 activation, *Cell Metab*, 2010, **12**(6), 662–667.

38 Yu W, Dittenhafer-Reed K E and Denu J M, SIRT3 protein deacetylates isocitrate dehydrogenase 2 (IDH2) and regulates mitochondrial redox status, *J Biol Chem*, 2012, **287**(17), 14078–14086.

39 Jacobs K M, Pennington J D, Bisht K S, Aykin-Burns N, Kim H S, *et al*., SIRT3 interacts with the daf-16 homolog FOXO3a in the mitochondria, as well as increases FOXO3a dependent gene expression, *Int J Biol Sci*, 2008, **4**(5), 291–299.

40 Sundaresan N R, Gupta M, Kim G, Rajamohan S B, Isbatan A, *et al*., Sirt3 blocks the cardiac hypertrophic response by augmenting Foxo3a-dependent antioxidant defense mechanisms in mice, *J Clin Invest*, 2009, **119**(9), 2758–2771.